Critical collapse of collisionless matter: A numerical investigation

Gerhard Rein
Mathematisches Institut der Universität München, Theresienstrasse 39, 80333 München, Germany

Alan D. Rendall
Max-Planck-Institut für Gravitationsphysik, Schlaatzweg 1, 14473 Potsdam, Germany

Jack Schaeffer
Department of Mathematics, Carnegie-Mellon University, Pittsburgh, Pennsylvania 15213
(Received 20 April 1998; published 10 July 1998)

In recent years the threshold of black hole formation in spherically symmetric gravitational collapse has been studied for a variety of matter models. In this paper the corresponding issue is investigated for a matter model significantly different from those considered so far in this context. We study the transition from dispersion to black hole formation in the collapse of collisionless matter when the initial data is scaled. This is done by means of a numerical code similar to those commonly used in plasma physics. The result is that, for the initial data for which the solutions were computed, most of the matter falls into the black hole whenever a black hole is formed. This results in a discontinuity in the mass of the black hole at the onset of black hole formation. [S0556-2821(98)02616-2]

PACS number(s): 04.20.Dw, 04.20.Ex, 04.25.Dm

I. INTRODUCTION

The gravitational collapse of a localized concentration of matter to a black hole is a central theme in general relativity. Even in the simplest case of spherically symmetric collapse much remains to be learned. When no matter is present, i.e. in the case of the vacuum Einstein equations, there is no collapse in spherical symmetry, because of Birkhoff's theorem. Thus it is necessary, in order to obtain information about gravitational collapse by studying the spherically symmetric case, to choose a matter model. A simple choice, which has provided valuable insights, is that of a massless (real, minimally coupled) scalar field. A deep mathematical investigation of spherically symmetric solutions of the Einstein-scalar field system has been carried out by Christodoulou. Some of his results will now be discussed.

In [1] it was shown that for sufficiently small initial data the fields disperse to infinity at large times. A result for the case of large data was proved in [2]. For any solution it is possible to define a number M with the property that in the region $r>2M$ (where r is the area radius) the solution approaches the Schwarzschild solution of mass M at large times. The physical interpretation is that the system has collapsed to form a black hole of mass M. Of course $M=0$ in the case that the field disperses. The dichotomy between dispersion and black hole formation still leaves the unanswered question of which data result in which of these two outcomes, except for small data. In [3] Christodoulou gave a sufficient condition on initial data to ensure that $M>0$ for the corresponding solution, although this criterion is not very practical.

For large data the above results only describe the structure of the solution at a sufficiently large radius and the internal structure is left open. In [4] it was proved that there exist data leading to the formation of a naked singularity. The negative implications of this for the cosmic censorship hypothesis are limited by the fact [5] that this behavior is unstable in the class of spherically symmetric initial data.

An important new element was brought into the study of the Einstein-scalar field and gravitational collapse in general by the numerical work of Choptuik [6]. He took a fixed initial datum for the scalar field (which due to spherical symmetry determines initial values for the gravitational field) and scaled it by an arbitrary constant factor. This gives rise to a family of initial data depending on a real parameter A. For all initial data used in the computations the same picture emerged. For values of A corresponding to small data the field dispersed, in agreement with the rigorous results. For large initial data a black hole was formed. Under these circumstances we can define a critical parameter A_* as the lower limit of those values of A for which a black hole is formed. If the mass M of the black hole formed is plotted as a function of A it is found that $M(A)$ is continuous. In particular $\lim_{A\to A_*} M(A)=0$ so that black holes of arbitrarily small mass can be formed within the given one-parameter family. Up to now it has not been possible to confirm this behavior by rigorous mathematical arguments. Choptuik's results contain much more detailed statements than the one just mentioned, but it is the one which will be important in the sequel.

The nature of the boundary between dispersion and black hole formation in gravitational collapse is now a very active research area. Most (but not all) of the work has been concerned with spherical symmetry and varying matter models and has relied essentially on numerical computations. For a recent review of the field see [7]. In a study of critical collapse for the Einstein-Yang-Mills equations, Choptuik, Chmaj and Bizoń [8] have found both cases where $\lim_{A\to A_*} M(A)=0$ and $\lim_{A\to A_*, A>A_*} M(A)>0$. They call these cases type II and type I respectively, the terminology being motivated by an analogy to phase transitions in statis-

 © 1998 The American Physical Society

tical mechanics. They relate type I behavior in this system to the existence of the Bartnik-McKinnon solutions [9,10], which are static. (The models which had been considered previously, and which showed exclusively type II behavior, admit no regular static solutions.)

Almost all the matter models which have been considered up to now in the context of critical collapse are field theoretic in nature rather than phenomenological. The one exception is a perfect fluid with linear equation of state, which shows type II behavior. A phenomenological matter model whose collapse is of interest is collisionless matter described by the Vlasov equation. As will be described next, the spherical collapse of collisionless matter has been studied both analytically and numerically but the known results for this type of matter say little about the nature of critical collapse. The purpose of this paper is to begin the numerical investigation of critical collapse of collisionless matter.

In [11] it was shown that for sufficiently small initial data for collisionless matter the matter disperses to infinity at large times. Thus the analogue of Christodoulou's small data result holds for collisionless matter. The solutions are geodesically complete. Unfortunately, no analogue of his large data result is known is this case. The only result in that direction which has been proved is that there do exist initial data which develop singularities [12]. The proof proceeds by demonstrating the existence of initial data which contain trapped surfaces and applying the Penrose singularity theorem. A different kind of large data result, which is relevant to the numerical calculations of this paper, is that if data given on a hypersurface of constant Schwarzschild time gives rise to a solution which develops a singularity after a finite amount of Schwarzschild time, then the first singularity occurs at the center of symmetry [13]. An analogous result where Schwarzschild time is replaced by maximal slicing has also been proved [14].

It seems plausible that in those solutions which develop singularities black holes are usually formed. However there are no mathematical results on this and the convincing evidence for the formation of black holes is purely numerical. This is part of a large body of work due to Shapiro, Teukolsky and collaborators which goes far beyond the spherically symmetric case. Here only those results will be discussed which are directly relevant to this paper. In particular only results for spherical symmetry are covered. In [15–17] the collapse of various configurations of collisionless matter to a black hole has been computed numerically. The relative merits for this problem of different choices of time coordinate (polar or maximal) and radial coordinate (area or isotropic) are discussed in [18,19].

In this paper we carry out an experiment analogous to that of Choptuik for spherically symmetric collapse of collisionless matter. We use Schwarzschild coordinates (i.e. polar slicing and area radius). Starting with a suitable smooth function f_0 of compact support as initial datum for the distribution function we consider the scaled data Af_0, where A is a positive constant and compute the corresponding time evolution numerically. For all data for which we tried the experiment, the results were qualitatively similar. When A is sufficiently small the matter disperses, in agreement with the analytic theory. This happens up to some value A_* of A. For $A>A_*$ the observed behavior indicates the formation of a black hole. The lapse function develops an abrupt step at a certain radius $r(A)$. This step remains at the same radius but gets deeper and deeper. We interpret this as the signature of a black hole with mass $M(A)=r(A)/2$. If $M(A)$ is plotted as a function of A it is found that the limiting value of $M(A)$ as A approaches A_* from above is strictly positive. Thus we find behavior of type I in the terminology of [8]. We never find any signs of singularity formation for any value of A and this is consistent with the standard picture where the only singularities formed are those of black hole type and they are avoided by a Schwarzschild time coordinate.

As a check on the interpretation of the numerical solutions as describing collapse to a black hole, radial null geodesics were computed. The results agreed well with the expected picture. Radial null geodesics starting at the center at early times escape to large values of r. Those starting after a certain time T_1 remain within a finite radius. The limit of this radius as t tends to T_1 from above is equal to $r(A)$ as computed above. Thus we obtain a consistent picture with a black hole whose event horizon is generated by the null geodesics starting at the center at time T_1.

To have a better picture of what is happening in the collapse of near critical initial data it is useful to consider how the mass $M(A)$ of the black hole formed depends on the Arnowitt-Deser-Misner (ADM) mass of the initial configuration. For parameter values A well above A_* these quantities are almost equal. In other words, essentially all the matter falls into the black hole. As the critical parameter value is approached from above some of the matter does not fall into the black hole and in some of the cases which were computed escapes to infinity. However, in all the cases which were computed the mass of the black hole is more than 90% of the total ADM mass of the configuration. Thus whenever a black hole is formed almost all the matter falls into it and the mass gap is a reflection of this. The picture in the only other case of a phenomenological matter model in which critical collapse has been studied up to now, namely a perfect fluid with linear equation of state, is very different. In the case of a radiation fluid [equation of state $p=(1/3)\rho$] the slightly supercritical collapse can be described as follows [20]. The matter divides almost completely into two parts, separated by a near vacuum region. The outer part of the matter, which contains almost all the mass, escapes to infinity. The inner part, which contains only a very small amount of mass, collapses to form a (small) black hole. As the critical parameter is approached this situation becomes more and more extreme and the black hole mass tends to zero.

The numerical code used is based on a numerical scheme for the corresponding Newtonian problem described in [21]. It incorporates less refined features than the codes of Shapiro and Teukolsky but seems to be quite sufficient for the present task. It does have the advantage that an analogous Newtonian code has been proved to be convergent [21] and it seems reasonable to hope that this proof could be extended so as to obtain results on the convergence of the method used in this paper in the future.

These results add collisionless matter to the class of mat-

ter models for which something is known about critical collapse. Clearly it is desirable to examine other types of initial data so as to discover the prevalence of the type of behavior found here or of others which have not yet been seen. It is our hope that these numerical investigations can also help to further the mathematical study of collisionless matter in general relativity by providing pictures of what is happening which can suggest which theorems one should try to prove and by what means. Mathematical investigations of partial differential equations often proceed by estimating the growth rates of certain quantities and it is useful to have an idea of the expected growth rates on the basis of numerical computations. The fact that we observe no singularities in the numerical computations can be seen as evidence that the weak cosmic censorship conjecture is true for collisionless matter. Indeed it may even be true in a stronger version than in the case of the massless scalar field. There may be no naked singularities formed for any regular initial data rather than just for generic initial data. This speculation is based on the fact that the naked singularities which occur in scalar field collapse appear to be associated with the existence of type II critical collapse.

The paper proceeds as follows: In the next section we formulate the Vlasov-Einstein system, first in general coordinates, and then in coordinates adapted to the spherically symmetric, asymptotically flat situation that we want to study. In Sec. III we describe the code we are using and test it on a steady state. In Sec. IV we present the results of the numerical simulations.

II. FORMULATION OF THE SPHERICALLY SYMMETRIC VLASOV-EINSTEIN SYSTEM

In the present paper the matter model is a collisionless gas as described by the Vlasov or Liouville equation. Coupling this equation self-consistently to the Einstein field equations results in the Vlasov-Einstein system, which we first write down in general coordinates on the tangent bundle TM of the spacetime manifold M:

$$p^\alpha \partial_{x^\alpha} f - \Gamma^\alpha_{\beta\gamma} p^\beta p^\gamma \partial_{p^\alpha} f = 0,$$

$$G^{\alpha\beta} = 8\pi T^{\alpha\beta},$$

$$T^{\alpha\beta} = \int p^\alpha p^\beta f \, |g|^{1/2} \frac{d^4 p}{m}.$$

Here f is the number density of the particles on phase-space, $\Gamma^\alpha_{\beta\gamma}$ and $G^{\alpha\beta}$ denote the Christoffel symbols and the Einstein tensor obtained from the spacetime metric $g_{\alpha\beta}$, $|g|$ denotes its determinant, $T^{\alpha\beta}$ is the energy-momentum tensor generated by f, x^α are coordinates on M, (x^α, p^β) the corresponding coordinates on the tangent bundle TM, Greek indices run from 0 to 3, and

$$m = |g_{\alpha\beta} p^\alpha p^\beta|^{1/2}$$

is the rest mass of a particle at the corresponding phase-space point. We assume that all particles have rest mass 1 and move forward in time so that the distribution function f lives on the mass shell:

$$PM = \{ g_{\alpha\beta} p^\alpha p^\beta = -1, \; p^0 > 0 \}.$$

We consider this system in the asymptotically flat and spherically symmetric case and use Schwarzschild coordinates to coordinatize the spacetime manifold. The metric takes the form

$$ds^2 = -e^{2\mu(t,r)} dt^2 + e^{2\lambda(t,r)} dr^2 + r^2 (d\theta^2 + \sin^2\theta d\phi^2),$$

where $t \in \mathbb{R}$, $r \geqslant 0$, $\theta \in [0,\pi]$, $\phi \in [0,2\pi]$. Asymptotic flatness is then expressed as the boundary condition

$$\lim_{r\to\infty} \lambda(t,r) = \lim_{r\to\infty} \mu(t,r) = 0.$$

We also require a regular center, which is guaranteed by the boundary condition

$$\lambda(t,0) = 0.$$

To write the Vlasov equation we use the corresponding Cartesian coordinates

$$x = (r \sin\theta \cos\phi, r \sin\theta \sin\phi, r \cos\theta)$$

as spatial and

$$v^a = p^a + (e^\lambda - 1) \frac{x \cdot p}{r} \frac{x^a}{r}, \quad a = 1,2,3$$

as momentum coordinates. The Vlasov-Einstein system then takes the form

$$\partial_t f + e^{\mu-\lambda} \frac{v}{\sqrt{1+|v|^2}} \cdot \partial_x f - \left(\dot{\lambda} \frac{x \cdot v}{r} + e^{\mu-\lambda} \mu' \sqrt{1+|v|^2} \right) \frac{x}{r} \cdot \partial_v f = 0, \quad (2.1)$$

$$e^{-2\lambda}(2r\lambda' - 1) + 1 = 8\pi r^2 \rho, \quad (2.2)$$

$$e^{-2\lambda}(2r\mu' + 1) - 1 = 8\pi r^2 p, \quad (2.3)$$

$$\rho(t,r) = \rho(t,x) = \int \sqrt{1+|v|^2} f(t,x,v) \, dv, \quad (2.4)$$

$$p(t,r) = p(t,x) = \int \left(\frac{x \cdot v}{r} \right)^2 f(t,x,v) \frac{dv}{\sqrt{1+|v|^2}}. \quad (2.5)$$

Here $x, v \in \mathbb{R}^3$, $r = |x|$, $\cdot$ denotes the Euclidean dot product in $\mathbb{R}^3$, and $\dot{\lambda} = \partial\lambda/\partial t$ and $\mu' = \partial\mu/\partial r$. f is assumed to be spherically symmetric in the sense that

$$f(t,x,v) = f(t,Ax,Av), \quad A \in \mathrm{SO}(3).$$

Equations (2.2) and (2.3) are the 00- and 11-components of the field equations; it can be shown that for a solution of the above system also the remaining nontrivial components of the field equations hold. We state the 01-component explicitly, since it is used in our numerical scheme:

$$\dot{\lambda} = -4\pi r e^{\lambda+\mu} j, \tag{2.6}$$

where

$$j(t,r) = j(t,x) = \int \frac{x\cdot v}{r} f(t,x,v)\,dv. \tag{2.7}$$

This form of the spherically symmetric Vlasov-Einstein system is convenient for analytical work and has been used in [11,13]. For numerical work one wishes to use the symmetry explicitly in the Vlasov equation in order to reduce the latter's dimension. One set of independent variables to use is

$$r = |x|, \quad u = |v|, \quad \alpha = \cos^{-1}\frac{x\cdot v}{ru}.$$

However, an equivalent and more convenient set of variables is

$$r = |x|, \quad w = \frac{x\cdot v}{r}, \quad L = |x|^2|v|^2 - (x\cdot v)^2 = |x\times v|^2, \tag{2.8}$$

particularly because L is constant along the characteristics of (2.1); note that

$$u^2 = w^2 + \frac{L}{r^2}.$$

In these variables the Vlasov equation for $f = f(t,r,w,L)$ becomes

$$\partial_t f + e^{\mu-\lambda}\frac{w}{\sqrt{1+u^2}}\partial_r f - \left(\dot{\lambda} w + e^{\mu-\lambda}\mu'\sqrt{1+u^2} - e^{\mu-\lambda}\frac{L}{r^3\sqrt{1+u^2}}\right)\partial_w f = 0. \tag{2.9}$$

The field equations remain unaffected, and the source terms (2.4), (2.5), (2.7) can be rewritten in terms of (r,u,α) or (r,w,L).

We now mention some results that have been established for the spherically symmetric Vlasov-Einstein system. Throughout we consider as initial condition a spherically symmetric, nonnegative function $\overset{\circ}{f}$ which as a function of x and v is continuously differentiable, has compact support and satisfies the inequality

$$\int_{|x|\le r}\int \sqrt{1+v^2}\,\overset{\circ}{f}(x,v)\;dv\;dx < \frac{r}{2}, \quad r>0, \tag{2.10}$$

which means that the initial hypersurface does not contain a trapped surface. In [11] it was shown that for such an initial condition there exists a unique, continuously differentiable solution f with $f(0) = \overset{\circ}{f}$, which exists with respect to Schwarzschild time on some right maximal interval $[0,T[$. If the solution blows up in finite time, i.e., if $T<\infty$ then $\rho(t)$ becomes unbounded as $t\to T-$. Actually, as shown in [13], ρ in this case has to become unbounded at the center $r=0$, i.e., if any singularity evolves, the first one must be at the center. This rules out singularities of shell crossing type, which can be a nuisance in other matter models, e.g., dust. If the initial datum is uniformly small the resulting solution is global in the sense that the spacetime is geodesically complete and the components of the energy momentum tensor as well as metric quantities decay with certain algebraic rates in t.

Let us denote

$$m(t,r) = 4\,\pi\int_0^r s^2\rho(t,s)\;ds. \tag{2.11}$$

Then $m(t,\infty)$ is a conserved quantity, the ADM mass of the system. Using $m(t,r)$ the field equations (2.2) and (2.3) yield

$$e^{-2\lambda(t,r)} = 1 - \frac{2m(t,r)}{r}, \tag{2.12}$$

$$\mu'(t,r) = e^{2\lambda(t,r)}\left(\frac{m(t,r)}{r^2} + 4\pi r p(t,r)\right), \tag{2.13}$$

also

$$\lambda'(t,r) = \frac{1}{2r}[e^{2\lambda}(8\pi r^2\rho(t,r)-1)-1] = e^{2\lambda}\left(-\frac{m(t,r)}{r^2} + 4\pi r\rho(t,r)\right); \tag{2.14}$$

note that the right hand side of Eq. (2.12) is positive at $t=0$ by the assumption (2.10). A further quantity which is conserved by the system is the total number of particles

$$\int\int e^{\lambda} f(t,x,v)\;dv\;dx. \tag{2.15}$$

III. DESCRIPTION AND TESTING OF THE CODE

Let us consider an initial condition, $\overset{\circ}{f}(x,v)$, which is spherically symmetric, satisfies the condition (2.10), and vanishes outside the set $(r,u,\alpha)\in[R_0,R_1]\times[U_0,U_1]\times[\alpha_0,\alpha_1]$. We will approximate the solution using a particle method. For a thorough treatment of particle methods in the context of plasma physics see [22]. To generate the particles we take integers N_r, N_u, N_α and define

$$\Delta r = \frac{R_1-R_0}{N_r}, \quad \Delta u = \frac{U_1-U_0}{N_u}, \quad \Delta\alpha = \frac{\alpha_1-\alpha_0}{N_\alpha},$$

$$r_i = R_0 + \left(i-\frac{1}{2}\right)\Delta r, \quad u_j = U_0 + \left(j-\frac{1}{2}\right)\Delta u,$$

$$\alpha_k=\alpha_0+\left(k-\frac{1}{2}\right)\Delta\alpha,$$

$$f^0_{ijk}=\mathring{f}(r_i,u_j,\alpha_k)4\pi r_i^2\Delta r 2\pi u_j^2\Delta u\ \sin\ \alpha_k\Delta\alpha,$$

$$r^0_{ijk}=r_i,\ \ w^0_{ijk}=u_j\ \cos\ \alpha_k,\ \ L_{ijk}=(r_iu_j\ \sin\ \alpha_k)^2.$$

From these, approximations are made of the quantities ρ, p, j, and m defined in Eqs. (2.4), (2.5), (2.7), and (2.11) at the grid points $n\Delta r$. The equation

$$\mu'=\frac{1}{1-\dfrac{2m}{r}}\left(\frac{m}{r^2}+4\pi rp\right), \tag{3.1}$$

which is obtained from Eqs. (2.12) and (2.13), together with $\mu\to 0$ as $r\to\infty$ is used to compute μ on this grid. Note that for r outside the support, $p\equiv 0$ and $m\equiv$ constant and this equation is explicitly integrable. λ is computed using Eq. (2.12), and similarly $\dot{\lambda}$ and λ' are computed using Eqs. (2.6) and (2.14). Letting D denote differentiation along a characteristic of the Vlasov equation (2.9) we have

$$Dr=e^{\mu-\lambda}\frac{w}{\sqrt{1+u^2}},$$

$$Dw=-w\dot{\lambda}-e^{\mu-\lambda}\sqrt{1+u^2}\mu'+\frac{e^{\mu-\lambda}L}{r^3\sqrt{1+u^2}}$$

$$DL=0;$$

recall that

$$u^2=w^2+\frac{L}{r^2}.$$

We interpolate ρ, j, p, μ, λ, etc. to particle locations and use these equations to define r^1_{ijk} and w^1_{ijk} using a simple Euler time stepping method. Here r^1_{ijk} denotes an approximation of the radius of the characteristic at time Δt with $r=r_i$, $u=u_j$, $\alpha=\alpha_k$ at time 0.

We also have the equation

$$(\Delta t)^{-1}(f^1_{ijk}-f^0_{ijk})=-f^0_{ijk}(\dot{\lambda}+w\lambda' e^{\mu-\lambda}(1+u^2)^{-1/2})$$

which represents the time evolution of a volume element along a characteristic. One time step is now complete.

To test the code a steady state solution was generated. Following [23] we take

$$f(x,v)=\phi(E)$$

where

$$E=e^{\mu}\sqrt{1+|v|^2}$$

is the particle energy. For simplicity

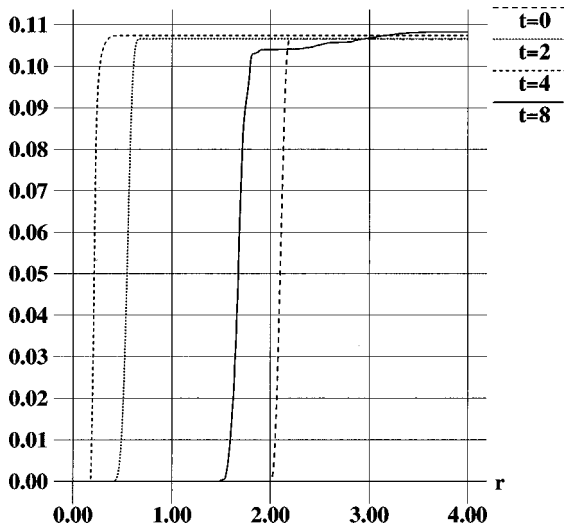

FIG. 1. Enclosed mass $m(r)$ for subcritical amplitude A.

$$\phi(E)=\begin{cases}1, & E<E_0\\ 0, & E\geqslant E_0\end{cases}$$

with $E_0>0$ was taken. Then from [23],

$$\rho(r)=g_\phi(\mu(r))$$

and

$$p(r)=h_\phi(\mu(r))$$

where

$$g_\phi(u)=4\pi\int_1^\infty\phi(\epsilon e^u)\epsilon^2\sqrt{\epsilon^2-1}\ d\epsilon$$

and

$$h_\phi(u)=\frac{4\pi}{3}\int_1^\infty\phi(\epsilon e^u)(\epsilon^2-1)^{3/2}d\epsilon.$$

Substituting into Eq. (3.1), μ must satisfy

$$\mu'(r)=\frac{1}{1-\dfrac{8\pi}{r}\displaystyle\int_0^r s^2g_\phi(\mu(s))\ ds}\times\left(\frac{4\pi}{r^2}\int_0^r s^2g_\phi(\mu(s))\ ds+4\pi rh_\phi(\mu(r))\right) \tag{3.2}$$

and $\mu\to 0$ as $r\to\infty$. This was solved using a shooting method. Note that for $\mu\geqslant\ln E_0$ (3.2) reduces to

$$\mu'(r)=\frac{r^{-2}m(\infty)}{1-2r^{-1}m(\infty)},$$

which is explicitly integrable. Thus, it was only necessary to solve (3.2) on a bounded domain. $E_0=0.9$ proved to be a convenient choice. The resulting steady state has mass 3.36×10^{-2} and support contained in $0\leqslant r\leqslant 0.36$. The radial component of v ranges from -0.64 to 0.64. The maximal values of μ and λ are 0.296 and 0.132 with ρ a decreasing function of r.

It was found that taking $N_r=40$, $N_u=10$, and $N_\alpha=10$ produced good results. This resulted in 2550 particles (less than $40\times10\times10$ since the support of f is not rectangular). At time zero the maximal errors in m and μ (maximum over r) were 1.63×10^{-4} and 2.84×10^{-3} respectively. Dividing by the maximal values of m and μ (that is, by 3.36×10^{-2} and 2.96×10^{-1}) we find the maximal errors in m and μ are 0.49% and 0.96% at $t=0$.

The errors in m and μ were computed at time $t=10$ using different time steps. Percentage errors were computed as described above with the results:

Δt	error in m	error in μ
$\frac{1}{4000}$	6.2%	5.9%
$\frac{1}{8000}$	3.4%	2.9%
$\frac{1}{16000}$	2.1%	1.3%

Thus the particle code tracks the steady state reasonably well, although a rather small time step seems to be needed. We attribute this, at least in part, to numerical difficulties in tracking the motion of particles near $r=0$. Note that for this steady state the density is largest at $r=0$. For other solutions with zero density near $r=0$, the time step was taken larger without significant change in the results.

IV. RESULTS OF SIMULATION

In this section we consider initial data

$$\mathring{f}(x,v)=Af_0(x,v)$$

with f_0 fixed and vary A. As a first example we take

$$f_0(x,v)=[50{,}000(2.2-r)(r-2)(10.2-u)\times(u-10)(3.1-\alpha)(\alpha-2.9)]^2$$

for $2<r<2.2$, $10<u<10.2$, $2.9<\alpha<3.1$ and $f_0(x,v)=0$ otherwise. Thus the mass is initially concentrated between $r=2$ and 2.2 and is moving inward rapidly. In most of the following simulations the support of f_0 is divided into 40 by 20 by 20 cells (40 in r) resulting in 16000 particles and the time step is 0.005. The cases where this is not so will be pointed out.

In Figs. 1 and 2, A is 0.69. In Fig. 1 the enclosed mass $m(t,r)$ defined in Eq. (2.11) is plotted at times $t=0$, 2, 4, and 8. Figure 2 shows μ at the same times. The solid curve is $t=8$ in both. At time 8 every particle is moving outward with momentum greater than 3.37 and has position $r>1.48$. In Fig. 1 we see that the mass has fallen inward and reversed

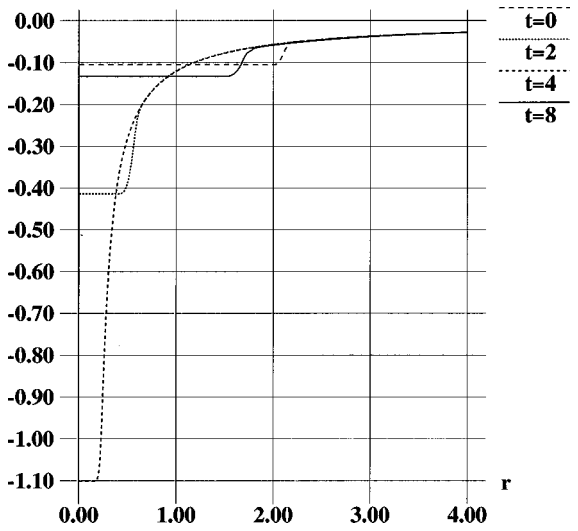

FIG. 2. $\mu(r)$ for subcritical amplitude A.

direction, almost returning to its starting position at time 8. Comparing Figs. 1 and 2 we see that at $t=4$ the mass is near $r=0$ and that $|\mu|$ attains relatively large values. By $t=8$ μ has dropped to near its starting values. As t grows the particles continue outward and disperse, consistent with the small data result [11].

In Figs. 3 and 4, A is 0.75. Again m and μ are plotted at times $t=0$, 2, 4, and 8 with the solid curve representing $t=8$. For times 0, 2, and 4 Fig. 3 resembles Fig. 1, but for $t=8$ we see in Fig. 3 that the mass has not moved back out. Rather it is centered near 0.21, and from Fig. 4 μ has formed an abrupt transition near 0.235. At time 8 the maximal outward momentum is about 9 while the maximal inward momentum is 189 and the positions satisfy $0.13<r<0.24$. Examination of $j(t,r)$ defined in Eq. (2.7) reveals that the mass flux is almost entirely inward. The abrupt transition in μ occurs at $r=0.235$ and λ has a maximum at this same r. λ forms a cusp at its maximum. At time 16 these features have not moved although the maximal value of $|\mu|$ has grown.

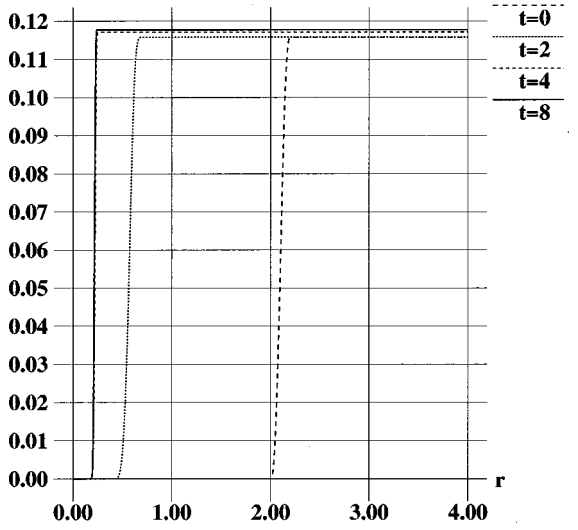

FIG. 3. Enclosed mass $m(r)$ for supercritical amplitude A.

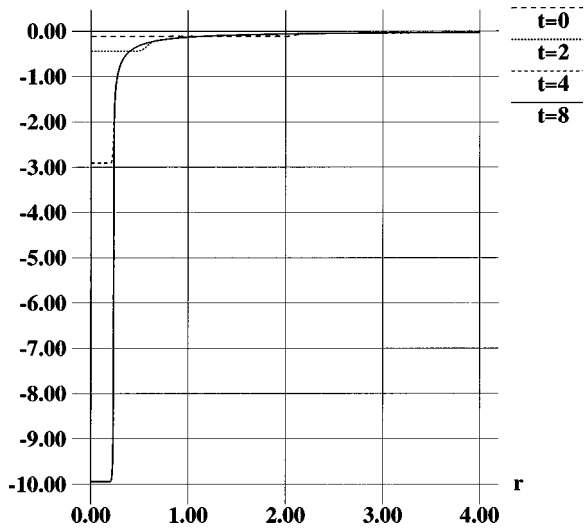

FIG. 4. $\mu(r)$ for supercritical amplitude A.

Recall that the quantities

$$\int \int e^{\lambda} f dv\ dx$$

and

$$\int \int \sqrt{1+|v|^2} f dv\ dx$$

are both conserved by the exact time evolution. In the above runs neither quantity varied by more than 1.7% of its initial value. A run was made with $80\times40\times40$ particles, $\Delta t = 0.0025$, $A=0.75$, and final time 8. The resulting graphs of m and μ with the finer resolution are qualitatively very similar to Figs. 3 and 4, except that the transitions are slightly more abrupt and the maximal value of $|\mu|$ is increased by about 7%.

When A was taken larger than 0.75 the results are similar. For $0.70 \leqslant A \leqslant 0.74$ a similar structure formed with a stationary abrupt transition in μ, but a small amount of mass escaped. Thus it seems that the critical value of A for this choice of f_0 is $A_* \approx 0.70$.

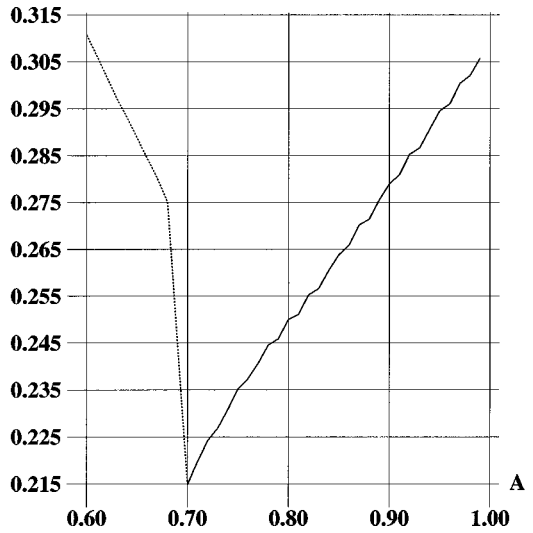

FIG. 5. Critical radius versus amplitude; first example.

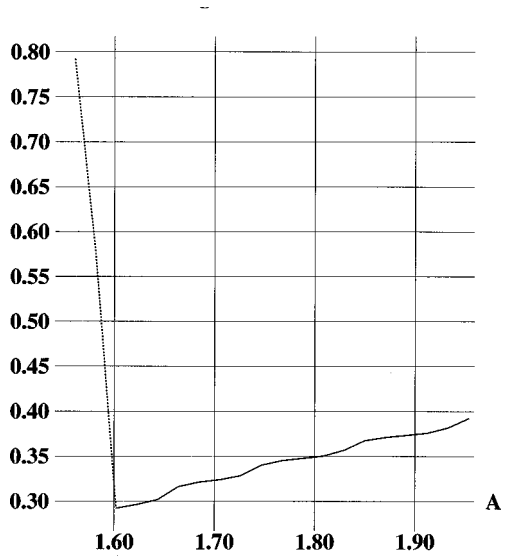

FIG. 6. Critical radius versus amplitude; second example.

For $A \geqslant 0.70$ the radius of the maximum of λ and the radius of the abrupt transition in μ are nearly the same. Thus we have computed the radius $r(A)$ where the maximal value (over r and t) of

$$\lambda = -\frac{1}{2}\ln\left(1-\frac{2m}{r}\right)$$

occurred. So this is the value of r where the condition (2.10) is most nearly violated. For $A \geqslant 0.70$ the maximum λ was attained at the largest time, for $A \leqslant 0.69$ it was attained earlier. The results are graphed in Fig. 5. Since the ADM mass of the configuration depends linearly on A and for $A \geqslant 0.70$ nearly all the mass is captured in the black hole, the mass of the black hole, $M(A)=r(A)/2$, depends nearly linearly on A for $A \geqslant 0.70$. The values of $A < 0.70$ are plotted as a dotted curve. We note that

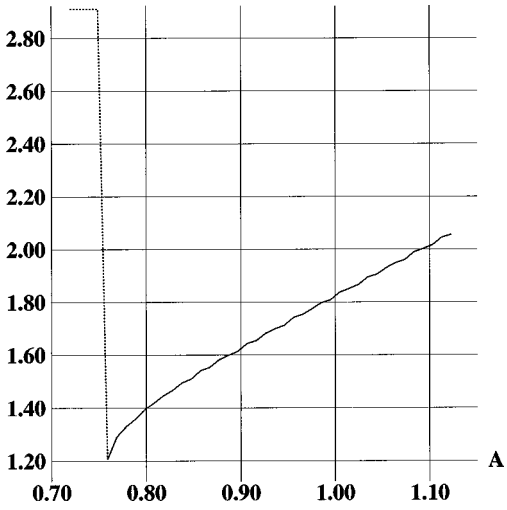

FIG. 7. Critical radius versus amplitude; third example.

$$\lim_{A\to A_*+} M(A) = \frac{1}{2} \lim_{A\to A_*+} r(A) \approx 0.11,$$

which indicates type I behavior as explained in the introduction. Since $\Delta r = 0.005$, the discontinuity in $M(A)$ at A_* is significant.

Next we consider

$$f_0(x,v) = 0.1(1-r^2)^2(1-u^2)^2$$

for $r<1$ and $u<1$ and $f_0(x,v)=0$ otherwise. Similar to Fig. 5, Fig. 6 shows the radius where the maximal value of λ occurs as a function of A. For $A \geqslant 1.6$ the maximum was attained at the largest time. For this initial condition a smaller time step of 0.00125 was used.

Similarly we consider

$$f_0(x,v) = 0.1(3-r)^2(2-r)^2(1-r)^2(1-u^2)^2$$

for $1<r<3$ and $u<1$ and $f_0(x,v)=0$ otherwise. Figure 7 plots radius versus A as Figs. 5 and 6 did. For $A \geqslant 0.76$ the maximum of λ occurred at the largest time. For $A \leqslant 0.75$ the maximum occurred at times near zero, hence the nearly constant values of r for $A \leqslant 0.75$.

In Figs. 5, 6 and 7 the final time was taken large enough that increasing it produced only minor changes. In each case we see that the radius at which λ is largest and the step in the lapse function $e^{2\mu}$ forms remains bounded away from zero.

ACKNOWLEDGMENT

One of the authors (A.D.R.) thanks Carsten Gundlach for helpful discussions.

[1] D. Christodoulou, Commun. Math. Phys. **105**, 337 (1986).
[2] D. Christodoulou, Commun. Math. Phys. **109**, 613 (1987).
[3] D. Christodoulou, Commun. Pure Appl. Math. **44**, 339 (1991).
[4] D. Christodoulou, Ann. Math. **140**, 607 (1994).
[5] D. Christodoulou, ''The instability of naked singularities in the gravitational collapse of a scalar field,'' report.
[6] M. W. Choptuik, Phys. Rev. Lett. **70**, 9 (1993).
[7] C. Gundlach, ''Critical phenomena in gravitational collapse,'' gr-qc/9712084.
[8] M. W. Choptuik, T. Chmaj, and P. Bizoń, Phys. Rev. Lett. **77**, 424 (1996).
[9] R. Bartnik and J. McKinnon, Phys. Rev. Lett. **61**, 141 (1988).
[10] J. A. Smoller, A. G. Wasserman, S.-T. Yau, and J. B. McLeod, Commun. Math. Phys. **143**, 115 (1991).
[11] G. Rein and A. D. Rendall, Commun. Math. Phys. **150**, 561 (1992).
[12] A. D. Rendall, Class. Quantum Grav. **9**, L99 (1992).
[13] G. Rein, A. D. Rendall, and J. Schaeffer, Commun. Math. Phys. **168**, 467 (1995).
[14] A. D. Rendall, Banach Centre Publications **41**, 35 (1997).
[15] S. L. Shapiro and S. A. Teukolsky, Astrophys. J. **298**, 34 (1985).
[16] S. L. Shapiro and S. A. Teukolsky, Astrophys. J. **298**, 58 (1985).
[17] S. L. Shapiro and S. A. Teukolsky, Astrophys. J. **307**, 575 (1986).
[18] L. I. Petrich, S. L. Shapiro, and S. A. Teukolsky, Phys. Rev. D **31**, 2459 (1985).
[19] L. I. Petrich, S. L. Shapiro, and S. A. Teukolsky, Phys. Rev. D **33**, 2100 (1986).
[20] C. R. Evans and J. S. Coleman, Phys. Rev. Lett. **72**, 1782 (1994).
[21] J. Schaeffer, Q. Appl. Math. **45**, 59 (1987).
[22] C. K. Birdsall and A. B. Langdon, *Plasma Physics via Computer Simulation* (McGraw-Hill, New York, 1985).
[23] G. Rein and A. D. Rendall, Ann. Inst. Henri Poincaré: Phys. Theor. **59**, 383 (1993).